CHARACTERIZING WHOLESOME AND UNWHOLESOME CHICKENS BY CIELUV COLOR DIFFERENCE

K. Chao, Y. R. Chen, F. Ding, D. E. Chan

ABSTRACT. *An automated poultry carcass inspection system will help the poultry processing industry to provide better chicken products for the consumer while minimizing potential economic losses. The objective of this research was to investigate the potential of a color-based sensing technique suitable for rapid automated inspection for wholesomeness of chickens in the visible region. Spectra, in the range of 400 to 867 nm, of veterinarian-selected carcasses, 400 wholesome and 332 unwholesome, were collected from a high-speed kill line using a visible/near-infrared spectrophotometer system. CIELUV color differences characterizing wholesome and unwholesome chicken samples were calculated as a simple distance formula and used to classify individual samples. Results showed that the greatest color differences occurred for waveband combinations at (508 nm, 426 nm), (560 nm, 426 nm), and (640 nm, 420 nm). Full-spectrum classification achieved accuracies of 85%, 86%, 84%, and 82% for wholesome validation samples, wholesome testing samples, unwholesome validation samples, and unwholesome testing samples, respectively. Using the (560 nm, 426 nm) waveband combination, classification accuracies of 91%, 92%, 90%, and 90% were achieved for wholesome validation samples, wholesome testing samples, unwholesome validation samples, and unwholesome testing samples, respectively. The potential of using CIELUV color differences to differentiate between wholesome and unwholesome chickens was demonstrated, and the straightforward calculation involved suggest that the method is suitable for rapid automated online sorting of chicken carcasses.*

Keywords. *Colorimetry, Food safety, Poultry, Spectroscopy.*

New inspection technologies are needed that can allow poultry plants to meet government food safety regulations efficiently and also increase competitiveness and profitability while meeting rising consumer demand. Consequently, the development of accurate, rapid, and non-invasive science-based technologies appropriate for operation on high-speed processing lines is of great importance for the poultry industry (FSIS-USDA, 2001). Due to successful food safety and quality monitoring applications in other food processing and production agriculture industries, researchers have been developing spectral imaging methods suited for the poultry processing industry. In particular, visible/near-infrared (Vis/NIR) spectroscopic technologies have been shown capable of distinguishing between wholesome and unwholesome poultry carcasses and detecting fecal contamination on poultry carcasses due to differences in skin and tissue composition. Chen and Massie (1993) used Vis/NIR measurements taken by a photodiode array spectrophotometer to classify wholesome and unwholesome chicken carcasses, and selected wavelengths at 570, 543, 641, and 847 nm based on linear regression for classification. Using Vis/NIR measurements of fecal contamination of poultry carcasses, Windham et al. (2003a) identified four key wavelengths via principal component analysis at 434, 517, 565, and 628 nm. Through single-term linear regression (STLR), an optimal ratio of 574 nm/588 nm was determined and used to achieve 100% detection of contaminates (Windham et al., 2003b). Chao et al. (2004) developed an on-line inspection system to measure the reflectance spectra of poultry carcasses in the visible to near-infrared regions between 431 and 944 nm. The instrument measured the spectra of veterinarian-selected carcasses running at speeds of 140 and 180 birds per min. Results showed that this Vis/NIR system can be used to differentiate between wholesome and unwholesome poultry carcasses at high speeds. These studies include significant findings for the use of spectral reflectance in the visible region, but have not utilized methods of analysis for sample color as perceived through human vision.

The International Commission for Illumination (CIE) has established a colorimetry system for identifying and specifying colors, and for defining color standards. Following the establishment of the CIE 1924 luminous efficiency function ($V\lambda$), the system of colorimetry was developed based on the principles of trichromacy and Grassmann's laws of additive color mixture (Fairchild, 1998). The concept of the colorimetry system is that any color can be matched by an additive mixture of three primary colors: red, green, and blue. Because there are three different types of color receptor cones in the eye, all the colors that humans see can be described by coordinates in a three-dimensional color space, which measures the relative stimulations to each type of cone. These coordinates are called tristimulus values and can be measured in color-matching experiments. The tristimulus

Article was submitted for review in June 2004; approved for publication by the Food & Process Engineering Institute Division of ASAE in March 2005.

Mention of trade names or commercial products is solely for the purpose of providing specific information and does not imply endorsement or recommendation by the USDA.

The authors are **Kuanglin Chao,** Research Scientist, **Yud-Ren Chen, ASAE Member Engineer,** Research Leader, USDA/ARS/ISL, Beltsville, Maryland; **Fujian Ding,** Post-Doctoral Scholar, University of Kentucky, Lexington, Kentucky; and **Diane Chan,** Agricultural Engineer, USDA/ARS/ISL, Beltsville, Maryland. **Corresponding author:** Kuanglin Chao, USDA/ARS/ISL, Building 303, BARC-East, 10300 Baltimore Ave., Beltsville, MD 20705-2350; phone: 301-504-8450; fax: 301-504-9466; e-mail: chaok@ba.ars.usda.gov.

values are the amounts of the three primary colors, which were used to achieve a match.

A system using broad-band primaries was formalized in 1931 by the CIE. Wavelength-by-wavelength measurement of tristimulus values for the visible spectrum produces the color-matching functions. The tristimulus values for a particular color are labeled (X, Y, Z) in the CIE 1931 system. The tristimulus values are extended such that they can be obtained for any given stimulus, defined by a spectral power distribution (SPD) (Williamson and Cummins, 1983). The SPD can be measured by a spectrophotometer. From the SPD both the luminance and the chromaticity of a color are derived to precisely describe the color in the CIE system.

The overall objective of this research was to investigate a quantitative, color-based method suitable for rapid automated online sorting of wholesome and unwholesome chickens. Specific objectives were to characterize wholesome and unwholesome chicken color in CIE color coordinates, and to calculate a simple numerical color difference for the classification of chicken samples as wholesome and unwholesome.

Materials and Methods

Spectral Measurement of Chicken Samples

Fresh chicken carcasses on a high-speed processing plant kill line running at 140 birds/min were identified on-site by an FSIS veterinarian to be either wholesome or unwholesome. Of the 732 total samples, 400 birds were identified as wholesome. The 332 unwholesome chickens were identified according to FSIS condemnation disposition criteria (i.e., exhibiting signs of systemic disease conditions) that may render the carcass and its parts adulterated.

Spectral measurements of the chicken samples were collected using an online poultry inspection system, after defeathering and prior to the evisceration process. An Andor DV401-BV (Andor Technology, Belfast, Northern Ireland) charge-coupled-device (CCD) system, consisting of a thermoelectrically cooled 1024 × 127 array detector, was controlled by in-house developed software modules to acquire chicken sample spectra. Chicken samples were illuminated by an external illumination assembly (Model 6000, Spectra-Physics, Stratford, Conn.) consisting of a 100-W quartz tungsten halogen (QTH) filament lamp and a condensing lens (*f*/1.8, 33-mm aperture) to collimate the QTH light. A focusing assembly (Model 77799, Spectra-Physics, Stratford, Conn.) was used to focus the collimated light at one end of a bifurcated fiber-optic probe (C Technologies, Inc., Cedar Knolls, N.J.). The probe consisted of two concentric groups of fiber-optic bundles. The fibers of the outer bundle transmitted the focused light to illuminate the chicken surface from a distance of 20 mm. The fibers of the inner optic bundle, each 100 μm in diameter, returned reflected light to the CCD detector.

Procedure

On the processing plant kill line, fresh chickens are moving at 140 birds per min. Inverted, the birds hang from shackles positioned 6 in. apart center-to-center. The FSIS veterinarian examined the exterior condition of the birds as they emerged from the defeathering process and just prior to the position of the online poultry inspection system. Upon identifying the condition of a sample bird, the veterinarian placed a color-coded pendant (yellow for unwholesome, green for wholesome) on the shackle of that sample. The pendant was detected by a sensor (Model QS30LDLQ, Banner Engineering Corp., Minneapolis, Minn.) mounted on the inspection system. This sensor was positioned to trigger spectral measurement as the sample bird passed through the presentation area in front of the fiber-optic probe. The probe was positioned to scan across the mid-breast area of the bird. The chicken spectrum was identified as either wholesome or unwholesome according to the pendant color and was saved into a database.

The inspection system was wavelength-calibrated using several emission peaks (435.84, 546.07, 640.23, and 724.52 nm) from a high-intensity mercury-neon lamp and resulted in spectral measurements consisting of 1024 data points in the spectral range of 400 to 867 nm with an interval of approximately 0.5 nm. Exposure time for the spectral measurements was 140 ms. Reference and background measurements were taken each day. To establish a spectrally flat, repeatable, high energy reference, a reference spectrum was collected by placing the fiber-optic probe 20 mm from a reflectance target composed of 14-mm thick of polytetrafluoroethylene (Spectralon, Labsphere, Sutton, N.H.). A background measurement was taken to compensate for the zero energy signal using a black cylindrical Teflon sample cell with the light source turned off. Spectra were recorded as relative reflectance based on the Spectralon reference, according to the formula:

$$\text{Relative Reflectance} = \frac{\text{sample reflectance} - \text{background}}{\text{reference} - \text{background}} \quad (1)$$

CIELUV Color Difference Calculation

The color difference values in CIELUV color space between wholesome and unwholesome chicken sample spectra (400 to 700 nm) were calculated using the CIE tristimulus values *X*, *Y*, and *Z*. The CIE tristimulus values were obtained by multiplying the spectral irradiance of the QTH light source, S_λ (Wm^{-2} nm^{-1}), the spectral reflectance of the chicken samples, R_λ, and, as shown in figure 1, the 1931 CIE color matching functions $\bar{x}_\lambda$, $\bar{y}_\lambda$, and $\bar{z}_\lambda$:

$$\begin{aligned} X &= k\sum_\lambda S_\lambda R_\lambda \bar{x}_\lambda \\ Y &= k\sum_\lambda S_\lambda R_\lambda \bar{y}_\lambda \\ Z &= k\sum_\lambda S_\lambda R_\lambda \bar{z}_\lambda \end{aligned} \quad (2)$$

where *k* is a normalizing constant. The combined term of S_λ R_λ is called the spectral power distribution. In a special case where absolute values for the spectral power distribution is given, it is convenient to use k = 683 lumens per watt, from which the calculated value of *Y* is the luminous flux expressed in lumens.

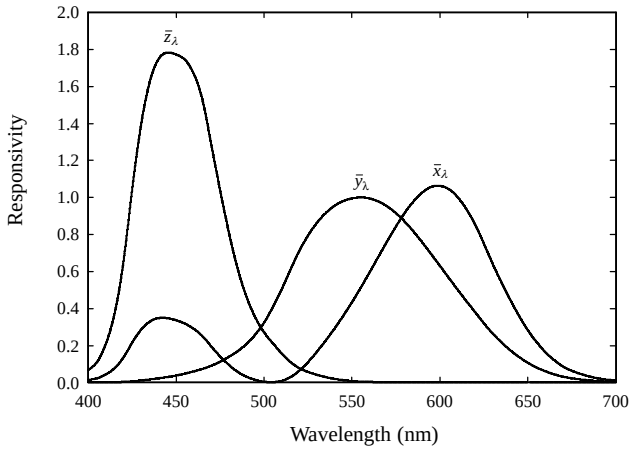

Figure 1. Spectral responsitivity of the CIE 1931 color matching functions.

The CIELUV color coordinates were calculated from the tristimulus values (Wyszecki and Stiles, 1982) as follows:

$$L^* = \begin{cases} 25\left(\frac{100Y}{Y_n}\right)^{1/3} - 16, & if\ \frac{Y}{Y_n} > 0.00856 \\ 903.29\left(\frac{Y}{Y_n}\right), & otherwise \end{cases} \quad (3)$$

$$u^* = 13L^*\left(u' - u'_n\right)$$

$$v^* = 13L^*\left(v' - v'_n\right)$$

with

$$u' = \frac{4X}{X + 15Y + 3Z}$$

$$v' = \frac{9Y}{X + 15Y + 3Z}$$

$$u'_n = \frac{4X_n}{X_n + 15Y_n + 3Z_n}$$

$$v'_n = \frac{9Y_n}{X_n + 15Y_n + 3Z_n}$$

The tristimulus values (X_n, Y_n, Z_n) were those of the white Spectralon reference target, for which the spectral reflectance was set to 1.0 for all wavelengths.

The additive nature of the tristimulus values, as seen in equation 2, means that for the mixing of colors, the tristimulus values X_i, Y_i, Z_i of the new color can be calculated from the tristimulus values of the j colors being mixed:

$$\begin{aligned} X_i &= X_1 + X_2 + ... + X_j \\ Y_i &= Y_1 + Y_2 + ... + Y_j \\ Z_i &= Z_1 + Z_2 + ... + Z_j \end{aligned} \quad (4)$$

The color difference index, ΔE, takes into account the difference in lightness, hue, and saturation between wholesome and unwholesome chicken samples and is calculated as the Euclidean distance between two points in the three-dimensional CIELUV space:

$$\Delta E\left(L^*u^*v^*\right) = \left[\left(\Delta L^*\right)^2 + \left(\Delta u^*\right)^2 + \left(\Delta v^*\right)^2\right]^{1/2} \quad (5)$$

Color differences between wholesome and unwholesome chicken samples in CIELUV color space were used to determine potential waveband pairs useful for classification. The tristimulus values for 10-nm wavebands centered at λ_1 and λ_2 were first calculated using equation 2 in the visible spectrum (400-700 nm). Using equation 4, the tristimulus values for color-mixing of all possible pairs of λ_1 and λ_2 were calculated. The color difference index ΔE was calculated for each of the 90,000 possible waveband combinations.

Classification Modeling

The classification model was created based on the color difference index, ΔE. The spectral data collected for 400 wholesome chickens and 332 unwholesome chickens was divided into a validation set and a testing set, each consisting of 200 wholesome and 166 unwholesome spectra. The tristimulus values X_{wref}, Y_{wref}, and Z_{wref} were obtained using the mean spectrum of the 200 wholesome validation spectra, and the tristimulus values X_{uref}, Y_{uref}, and Z_{uref} were obtained using the mean spectrum of the 166 unwholesome validation spectra. From these values, L^*_{wref}, u^*_{wref}, v^*_{wref} (for wholesome) and L^*_{uref}, u^*_{uref}, and v^*_{uref} (for unwholesome) were calculated. These coordinates in CIELUV space represent the reference points for wholesome and unwholesome chicken samples.

The values of L^*, u^*, and v^* for each of the individual 200 wholesome and 166 unwholesome spectra in the validation set were similarly calculated. With these values, the ΔE could be calculated between each sample and the wholesome and unwholesome reference points. The ΔE values between each sample and the wholesome and unwholesome reference points, d_1 and d_2, respectively, were calculated as:

$$d_1 = \left[\left(L^* - L^*_{wref}\right)^2 + \left(u^* - u^*_{wref}\right)^2 + \left(v^* - v^*_{wref}\right)^2\right]^{1/2} \quad (6)$$

$$d_2 = \left[\left(L^* - L^*_{uref}\right)^2 + \left(u^* - u^*_{uref}\right)^2 + \left(v^* - v^*_{uref}\right)^2\right]^{1/2} \quad (7)$$

A sample was classified as wholesome if $d_1 < d_2$ and as unwholesome if $d_1 \geq d_2$. These classification rules were also used to classify wholesome and unwholesome samples in the independent testing set.

A classification model was developed, as described above, using full-spectrum (400 nm – 700 nm) data, and also using selected pairwise combinations of 10-nm wavebands. For wavebands centered at λ_1 and λ_2, the tristimulus values $X_{\lambda 1}$, $Y_{\lambda 1}$, $Z_{\lambda 1}$ and $X_{\lambda 2}$, $Y_{\lambda 2}$, $Z_{\lambda 2}$ were calculated from mean wholesome and unwholesome spectra. The sum of these values, $X_{ref} = X_{\lambda 1} + X_{\lambda 2}$, $Y_{ref} = Y_{\lambda 1} + Y_{\lambda 2}$, $Z_{ref} = Z_{\lambda 1} + Z_{\lambda 2}$, were used to obtain the reference L^*, u^*, v^* values for wholesome and unwholesome birds. Similarly, for each sample in the validation and testing sets, tristimulus values for the mixing

of the two wavebands were used to obtain the L^*, u^*, v^* values for d_1 and d_2 calculation.

Results and Discussion

The average reflectance spectra of wholesome and unwholesome chicken samples are shown in figure 2. The relative reflectance is higher for wholesome samples than for unwholesome throughout the spectral range. The ΔE color difference values calculated for each individual wavelength from the mean wholesome and unwholesome spectra are shown in figure 3. Because the values were calculated at each for individual wavelength, lightness L^* was the only factor in determining these ΔE values. While the ΔE values are generally high across the spectrum, several distinctive features occur in the region between 430 and 600 nm. Figure 3 shows peaks near 445, 512, 558, and 588 nm, which correspond to spectral features in figure 2 that are characteristic of chicken spectra and known to show variation with different chicken conditions (Windham et al., 2003a; Chao et al., 2003).

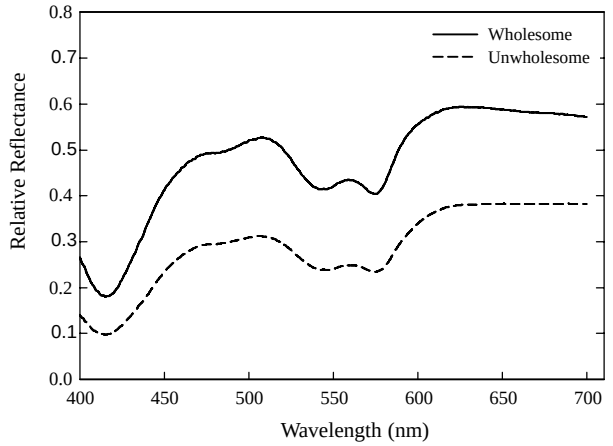

Figure 2. Mean spectra of wholesome and unwholesome chicken samples.

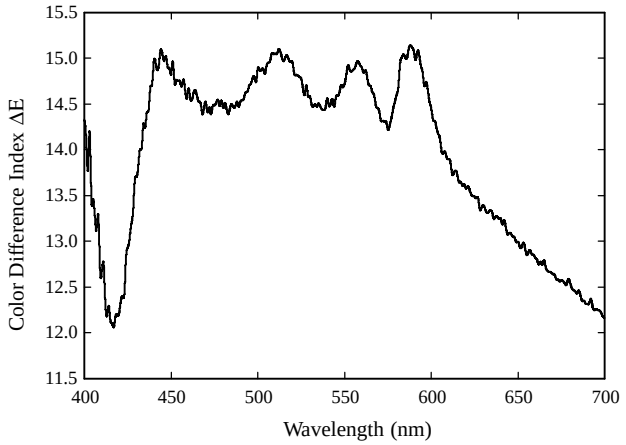

Figure 3. Wavelength-by-wavelength color difference between mean wholesome and unwholesome chicken spectra.

For well-bled samples such as those used in this study, the relative amounts of three forms of the pigment myoglobin are primarily responsible for the color of chicken meat and skin (Swatland, 1989; Liu and Chen, 2000a; Windham et al., 2003a). Deoxymyoglobin, metmyoglobin, and oxymyoglobin coexist and interconvert or degrade through oxidation and reduction reactions. Deoxymyoglobin has been associated with wavebands near 430, 440, and 455 nm; metmyoglobin with 485, 495, 500, and 505 nm; and oxymyoglobin with 545, 560, and 575 nm (Liu and Chen, 2000b). In general, wholesome and unwholesome chicken can be characterized by the relative amounts of these myoglobin forms, with wholesome chicken containing more oxymyoglobin and deoxymyoglobin, and unwholesome chicken containing more metmyoglobin (Liu and Chen, 2001).

Figure 4 shows a contour plot for the ΔE color difference values between mean wholesome and unwholesome chicken spectra, calculated for the 90,000 possible pairwise combinations of 10-nm wavebands centered at λ_1 and λ_2. In this case, given the color-mixing of the two wavebands, the ΔE values are determined by u^* and v^*, indicators of chromaticity, as well as by lightness L^*. Because the contour plot is symmetric about the diagonal, only the lower half of the plot is discussed here. An area of distinctly high ΔE values occurs in figure 4 where the λ_2 wavebands near 426 nm are combined with λ_1 wavebands between 475 and 660 nm. The λ_1 wavebands in this area correspond to the spectral region of high ΔE values in figure 3. In particular, peak ΔE values occur at the following waveband pairs of (λ_1, λ_2): (508 nm, 426 nm), (560 nm, 426 nm), and (640 nm, 420 nm). These waveband pairs were therefore selected as potentially useful color-mixing bands for ΔE classification models.

Figure 5 shows the results of the ΔE classification model based on full-spectrum wholesome and unwholesome chicken data. The classification results for wholesome samples in the validation data set are shown in section (a), for wholesome samples in the testing data set are shown in section (b), for unwholesome samples in the validation set are shown in section (c), and for unwholesome samples in the testing set are shown in section (d). Each sample is plotted according to its (d_1, d_2) coordinates, where d_1 and d_2 are the distances from the sample to the wholesome reference point and unwholesome reference point, respectively. Samples

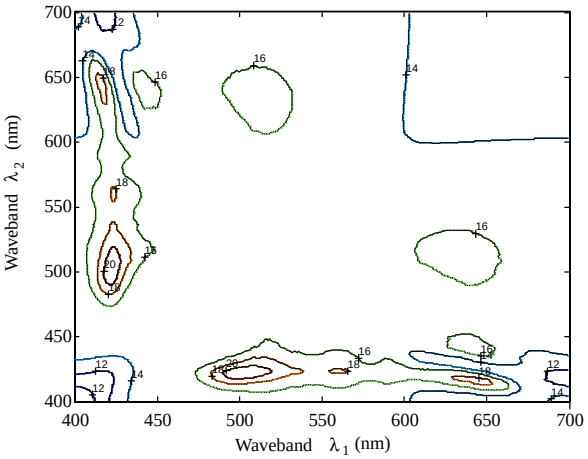

Figure 4. Contour plot of color difference between mean wholesome and unwholesome chicken spectra for waveband pairs.

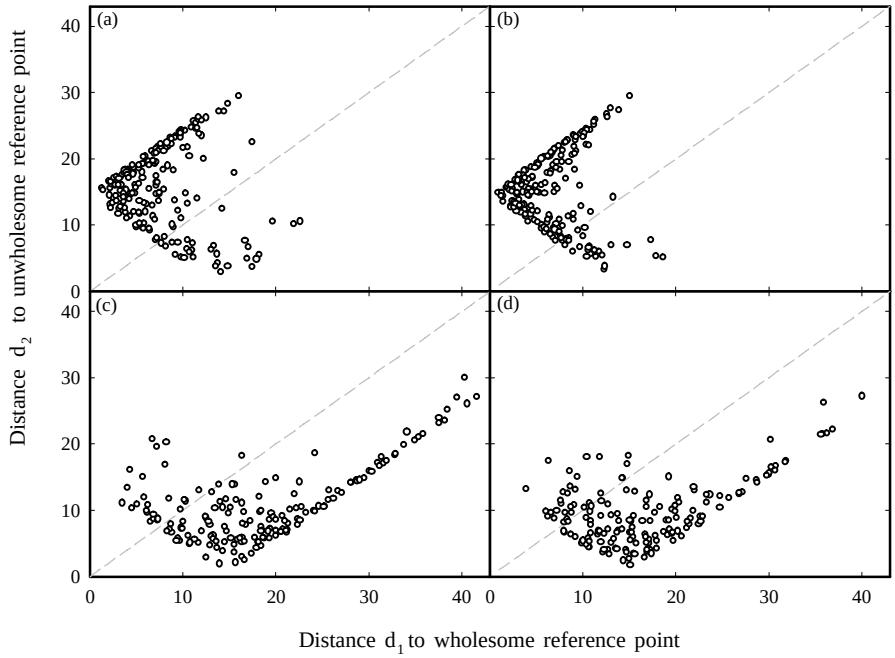

Figure 5. Plot of sample distance d_1, d_2 for full-spectrum classification of: (a) wholesome validation data; (b) wholesome testing data; (c) unwholesome validation data; (d) unwholesome testing data. Type I error is shown in the lower triangle of (a) and (b); Type II error is shown in the upper triangle of (c) and (d).

classified as wholesome fall above the diagonal, and samples classified as unwholesome fall below the diagonal. The classification accuracy achieved was 85% for wholesome validation samples (170 out of 200); 86% for wholesome testing samples (172 out of 200); 84% for unwholesome validation samples (140 out of 166); and 82% for unwholesome testing samples (136 out of 166).

Figures 6, 7, and 8 show the results of the ΔE classification models based on the 10-nm waveband pairs centered at (508 nm, 426 nm), (560 nm, 426 nm), and (640 nm, 420 nm), respectively, that were selected using the peaks from figure 4. For the (508 nm, 426 nm) waveband pair, 86% of wholesome validation samples, 87% of wholesome testing samples, 85% of unwholesome validation samples, and 86% of unwholesome testing samples were correctly classified. For the (560 nm, 426 nm) waveband pair, 91% of wholesome validation samples, 92% of wholesome testing samples, 90% of unwholesome validation samples, and 90% of unwholesome testing samples were correctly classified. For the (640 nm, 420 nm) waveband pair, 80% of wholesome

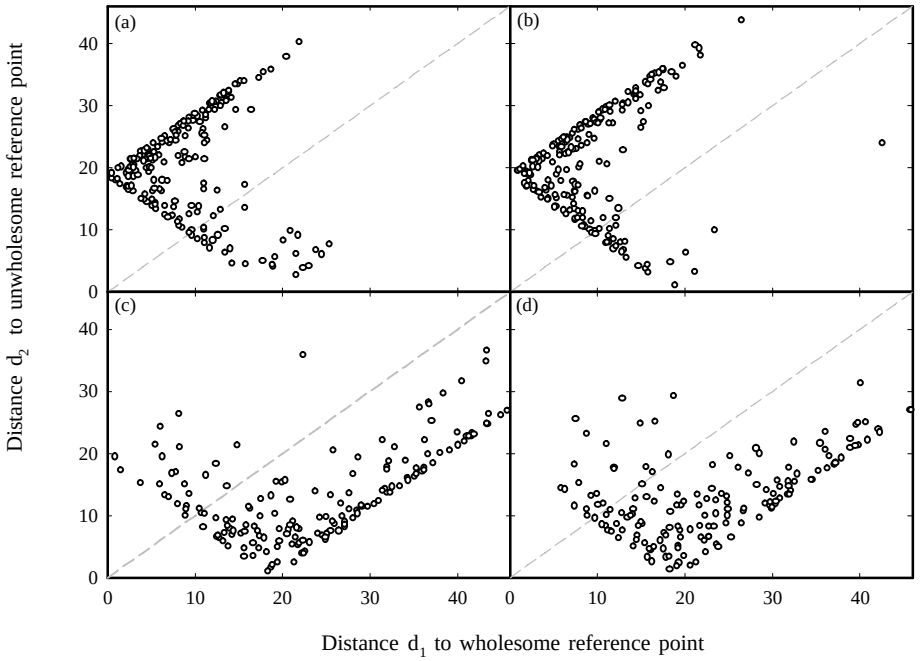

Figure 6. Plot of sample distance d_1, d_2 for waveband pair (508 nm, 426 nm) classification of: (a) wholesome validation data; (b) wholesome testing data; (c) unwholesome validation data; (d) unwholesome testing data. Type I error is shown in the lower triangle of (a) and (b); Type II error is shown in the upper triangle of (c) and (d).

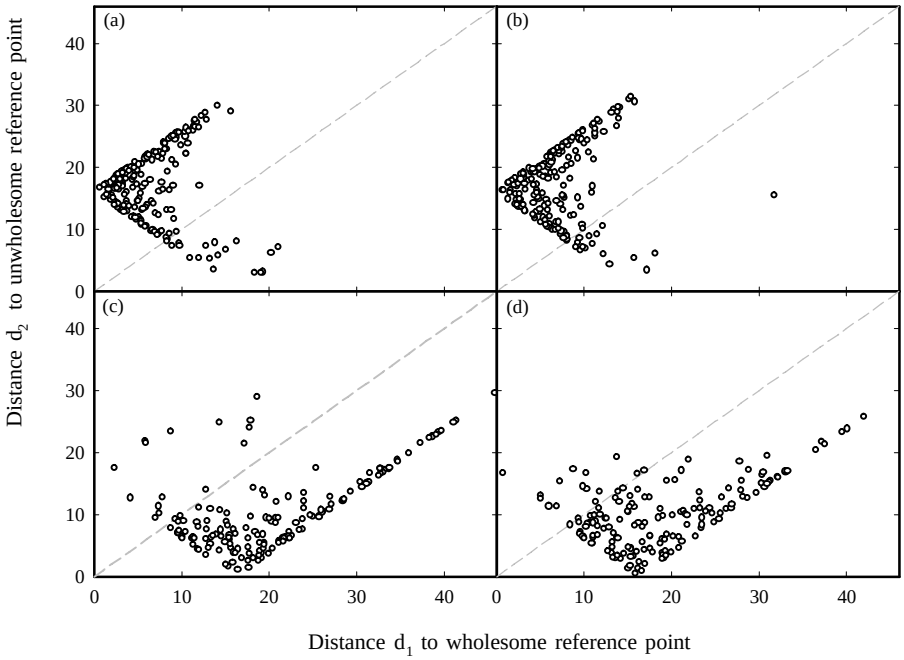

Figure 7. Plot of sample distance d_1, d_2 for waveband pair (560 nm, 426 nm) classification of: (a) wholesome validation data; (b) wholesome testing data; (c) unwholesome validation data; (d) unwholesome testing data. Type I error is shown in the lower triangle of (a) and (b); Type II error is shown in the upper triangle of (c) and (d).

validation samples, 79% of wholesome testing samples, 78% of unwholesome validation samples, and 77% of unwholesome testing samples were correctly classified. Table 1 summarizes these classification results.

The characteristic color differences between wholesome and unwholesome birds formed the basis for ΔE classification. No preprocessing of the raw spectral data, such as multiplicative scatter correction (MSC), spectral smoothing or second difference calculation was required before creating the ΔE classification models. The models used ΔE differences, by which simple distance calculations are reflecting inherent color differences of the samples. In comparison, more complex multivariate modeling approaches, such as partial least squares regression, are more sensitive to sample selection and calibration procedures, and can require more skilled interpretation beyond fundamental measures of sample characteristics.

The average testing accuracy of 91% achieved by the (560 nm, 426 nm) waveband pair outperformed the full-spectrum classification model, showing that selection of

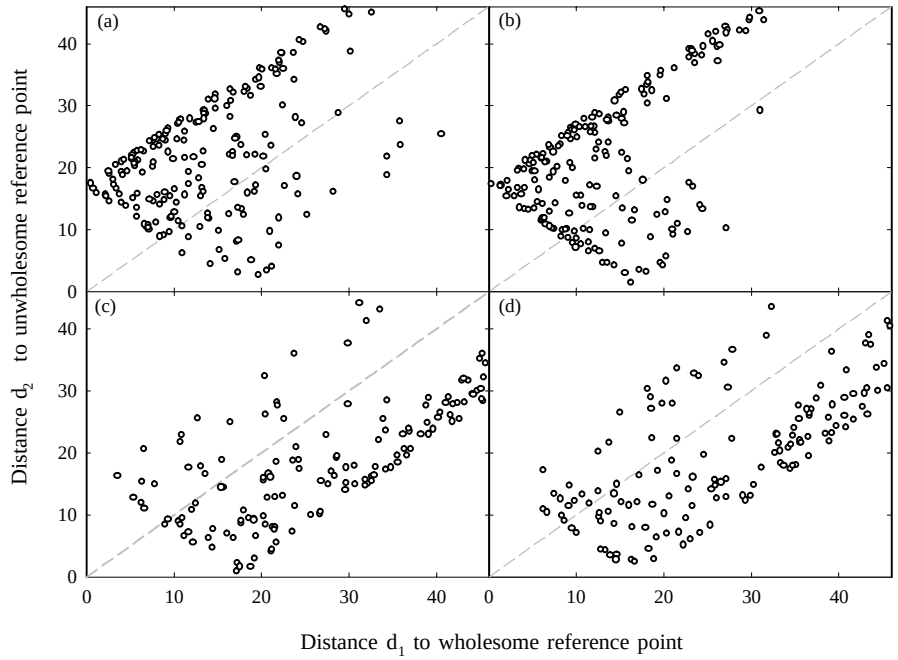

Figure 8. Plot of sample distance d_1, d_2 for waveband pair (640 nm, 420 nm) classification of: (a) wholesome validation data; (b) wholesome testing data; (c) unwholesome validation data; (d) unwholesome testing data. Type I error is shown in the lower triangle of (a) and (b); Type II error is shown in the upper triangle of (c) and (d).

Table 1. Fraction predicted correctly using the full spectrum and the three waveband pairs.

	Validation		Testing	
Model	Wholesome	Unwholesome	Wholesome	Unwholesome
Full spectrum	0.85	0.84	0.86	0.82
(508 nm, 426 nm)	0.86	0.85	0.87	0.86
(560 nm, 426 nm)	0.90	0.90	0.92	0.90
(640 nm, 420 nm)	0.80	0.78	0.79	0.77

wavebands in spectral regions related to myoglobin is useful for classification of wholesome and unwholesome chickens. Other studies have also found wavebands in myoglobin regions to be useful for poultry classification, such as the four dominant wavelengths of 434, 517, 565, and 628 nm for detection of fecal contamination on poultry carcasses (Windham et al., 2003b). The reasonably high accuracy achieved using only two wavebands suggests that reflectance measurements from the entire visible spectral region are not necessary for successful classification. Consequently, the ΔE color difference method could be implemented to classify wholesome and unwholesome chickens using two interference filters in instrumentation less costly than the full-spectrum instrument used for this study.

Summary and Conclusions

Spectral measurements were acquired for fresh chickens on a high-speed kill line. Significant CIELUV color difference values, calculated at each wavelength between the mean wholesome and unwholesome spectra, occurred near wavebands that have been associated with deoxymyoglobin, oxymyoglobin, and metmyoglobin in previous studies. Among all pairwise combinations of 10-nm wavebands between 400 and 700 nm, the greatest color difference values occurred for (508 nm, 426 nm), (560 nm, 426 nm), and (640 nm, 420 nm). Classification by color difference was calculated as a simple formula in CIELUV color space. Full-spectrum classification resulted in classification accuracies of 85%, 86%, 84%, and 82% for wholesome validation samples, wholesome testing samples, unwholesome validation samples, and unwholesome testing samples, respectively. The (560 nm, 426 nm) waveband combination showed the best classification, with accuracies of 91%, 92%, 90%, and 90% for wholesome validation samples, wholesome testing samples, unwholesome validation samples, and unwholesome testing samples, respectively. Since the numerical color difference is a very simple distance calculation and relatively highly classification accuracies can be achieved without full-spectrum data, this method shows promise for rapid automated online sorting of chicken carcasses.

References

Chao, K., Y. R. Chen, and D. E. Chan. 2003. Analysis of Vis/NIR spectral variations of wholesome, septicemia, and cadaver chicken samples. *Applied Engineering in Agriculture* 19(4): 453-458.

Chao, K., Y. R. Chen, and D. E. Chan. 2004. A spectroscopic system for high-speed inspection of poultry carcasses. *Applied Engineering in Agriculture* 20(5): 683-690.

Chen, Y. R., and D. R. Massie. 1993. Visible/near infrared reflectance and interactance spectroscopy for detection of abnormal poultry carcasses. *Transactions of the ASAE* 36(3): 863-889.

Fairchild, M. D. 1998. *Color Appearance Models*. Reading, Mass.: Addison Wesley.

Liu, Y., Y. R. Chen, and Y. Ozaki. 2000a. Characterization of visible spectral intensity variations of wholesome and unwholesome chicken meats with two-dimensional correlation spectroscopy. *Appl. Spectr.* 54(4): 587-594.

Liu, Y., and Y. R. Chen. 2000b. Two-dimensional correlation spectroscopy study of visible and near-infrared spectral variations of chicken meats in cold storage. *Appl. Spectr.* 54(10): 1458-1470.

Liu, Y., and Y. R. Chen. 2001. Analysis of visible reflectance spectra of stored, cooked, and diseased chicken meats. *Meat Sci.* 58(4): 395-401.

Swatland, H. J. 1989. A review of meat spectrophotometry (300 to 800 nm). *Can. Inst. Food Sci. Technol. J.* 22: 390-402.

USDA. 2001. FSIS strategic plan for fiscal years 2000-2005. Washington, D.C.: FSIS, USDA. http://www.fsis.usda.gov/om/planning/sp2005.htm. Last accessed 24 February 2005.

Williamson, S. J., and, H. Z. Cummins. 1993. *Light and Color in Nature and Art.* New York: Wiley.

Windham, W. R., K. C. Lawrence, B. Park, and R. J. Buhr. 2003a. Visible/NIR spectroscopy for characterizing fecal contamination of chicken carcasses. *Transactions of the ASAE* 46(3): 745-751.

Windham, W. R., D. P. Smith, B. Park, K. C. Lawrence, and P. W. Feldner. 2003b. Algorithm development with visible/near-infrared spectra for detection of poultry feces and ingesta. *Transactions of the ASAE* 46(6): 1733-1738.

Wyszecki, G., and W. S. Stiles. 1982. *Color Science: Concepts and Methods, Quantitative Data and Formulas*. New York: Wiley.